The impact of a hygroscopic chitosan coating on the controlled release behaviour of zinc hydroxide nitrate–sodium dodecylsulphate–imidacloprid nanocomposites

by Rahadian Zainul Et.al

Submission date: 20-May-2021 02:28PM (UTC+0700)
Submission ID: 1590159908
File name: Paper_Terbaru_Royal_Society_of_Chemistry_NJC.pdf (501.54K)
Word count: 9259
Character count: 43330

NJC

ROYAL SOCIETY OF CHEMISTRY

PAPER

Cite this: *New J. Chem.*, 2020, 44, 9097

The impact of a hygroscopic chitosan coating on the controlled release behaviour of zinc hydroxide nitrate–sodium dodecylsulphate–imidacloprid nanocomposites

Sharifah Norain Mohd Sharif,[a] Norhayati Hashim, *[ab] Illyas Md Isa,[ab] Suriani Abu Bakar,[c] Mohamad Idris Saidin,[a] Mohamad Syahrizal Ahmad,[a] Mazidah Mamat,[d] Mohd Zobir Hussein[e] and Rahadian Zainul[f]

Received 16th March 2020,
Accepted 11th May 2020

DOI: 10.1039/d0nj01315c

rsc.li/njc

Imidacloprid (IC) is a neutral charge insecticide that is commonly used in paddy cultivation areas to kill invasive insects. However, the uncontrolled usage of IC may cause serious problems for non-target organisms and the environment. This work focusses on the potential of using chitosan to develop an efficient insecticide that could minimise the environmental risk by controlling the release of IC into the environment. The powder X-ray diffraction (PXRD) and Fourier transform infrared (FTIR) analysis of the chitosan coated zinc hydroxide nitrate–sodium dodecylsulphate–imidacloprid (ZHN–SDS–IC-Chi) nanocomposite confirmed that the chitosan coating process did not interfere with the types of ions that were intercalated in the interlayer gallery of the nanocomposite. The release study performed in aqueous solutions of Na_3PO_4, Na_2SO_4 and NaCl revealed that the slowest release was observed when using NaCl as the release media. The release of IC was governed by the pseudo second order kinetic model, which described the release mechanism of the IC as being via dissolution and ion exchange. Even though the overall findings showed that the physicochemical properties of the ZHN–SDS–IC and ZHN–SDS–IC-Chi were not too different, the presence of chitosan was found to be beneficial for prolonging the release process. The synthesised ZHN–SDS–IC-Chi nanocomposite will hopefully be used as a safer insecticide in paddy cultivation and will fulfil both economic and ecological demands.

1. Introduction

It has long been recognised that controlled release technologies possess great potential in various sectors, including agricultural, pharmaceutical and food industries.[1–7] In the agricultural sector, the implementation of a controlled release formulation (CRF) into pesticides helps to prolong the release of the pesticide.[8,9] The excessive use of pesticides is not only costly, but also risky to the environment.[10,11] Therefore, the CRF in pesticides implies that the formulations involved are so created as to deliver the proper dosage for effective long or short term pest control. Pesticides integrated with CRF are an endeavour to develop the ideal delivery system of the pesticide and allow a sufficient release of the pesticide that will effectively exterminate pests while preserving the environment.[12] Releasing the pesticide in a slow and sustainable manner will assist in preventing environmental pollution by minimising the distribution of excess pesticide residues to the environment (via evaporation, degradation or leaching by rain into the waterway), which commonly occurs due to the simultaneous release of high pesticide concentrations.[13]

Zinc hydroxide nitrate (ZHN), with the general formula of $Zn_5(OH)_8(NO_3)_2\,2H_2O$, is amongst the attractive layered metal hydroxides that are commonly used as host materials in CRF. The positively charged ZHN provides an interlayer gallery of a flexible height that can contain a wide range of functional guest anions for CRF purposes, including cinnamate, 4-(2,4-dichlorophenoxy)butyrate, 2-(3-chlorophenoxy) propionate and 4-dichlorophenoxy acetate.[14–17] The anions accommodate the interlayer

[a] Department of Chemistry, Faculty of Science and Mathematics, Universiti Pendidikan Sultan Idris, 35900 Tanjong Malim, Perak, Malaysia. E-mail: norhayati.hashim@fsmt.upsi.edu.my; Fax: +60 15 4879 7296; Tel: +60 15 4879 7314
[b] Nanotechnology Research Centre, Faculty of Science and Mathematics, Universiti Pendidikan Sultan Idris, 35900 Tanjong Malim, Perak, Malaysia
[c] Department of Physics, Faculty of Science and Mathematics, Universiti Pendidikan Sultan Idris, 35900 Tanjong Malim, Perak, Malaysia
[d] School of Fundamental Science, Universiti Malaysia Terengganu, 21030 Kuala Terengganu, Terengganu, Malaysia
[e] Materials Synthesis and Characterization Laboratory, Institute of Advanced Technology, Universiti Putra Malaysia, 43400 Serdang, Selangor, Malaysia
[f] Department of Chemistry, Faculty of Mathematics and Natural Science, Universitas Negeri Padang, West Sumatera 25171, Indonesia

gallery and counterbalance the excessive positive charge generated by the ZHN and stabilise the overall charge. The intercalation of anions into the interlayer gallery of the ZHN, creates a host–guest nanocomposite that is favourable for CRF. Owing to its versatility, ZHN can also be intercalated with a neutral charge ion with the assistance of a surfactant.[8] The interaction between the host and guest ions significantly affects the CRF behaviour of the nanocomposite in terms of diffusion, release rate and other physicochemical properties.[12] A previous study showed that the intercalation of the guest ions was successfully performed via direct reaction, ion exchange and reconstruction methods.[4,17–20]

Although the potential of ZHN as an ideal host for CRF has been acknowledged, the delivery efficiency of the nanocomposite can be further improved by introducing a biopolymer material as a coating for the nanocomposite. Chitosan, a well-studied polysaccharide derived by partial N-deacetylation of chitin, is a potential coating for the pesticides with CRF due to its biodegradability, mucoadhesive properties, non-toxic nature, and ability to form a film and gel.[21,22] Free amino groups that are present in its structure make it insoluble in neutral or basic media. Hence, the use of an acid is needed to complete the solubilization so that the amino group can be protonated and the polymer can swell.[23] Chitosan was previously reported to be used in the controlled release of curcumin, aspirin, solid lipid nanoparticles and NPK fertilisers.[22,24,25] The incorporation of chitosan was also reported to enhance the thermal stability of the particular compound.[26] The chemical structure of chitosan is shown in Fig. 1.

Imidacloprid (IC) is a neonicotinoid, neutral charge insecticide that is widely used in paddy cultivation areas to kill invasive insects such as brown planthoppers, white-backed planthoppers and small brown planthoppers.[27] The chemical structure of IC is shown in Fig. 2. Similar to other neonicotinoid insecticides, IC penetrates into the central nervous system of these insects, and disturbs their nicotinic acetylcholine receptors.[28–30] Due to the neutral charge of IC, this insecticide may not be directly intercalated into the interlayer gallery of ZHN. However, our recently published paper has reported on the possibility of intercalating IC into ZHN with the assistance of sodium dodecylsulphate (SDS), by creating a hydrophobic region in the interlayer gallery, thus assisting the intercalation process.[31]

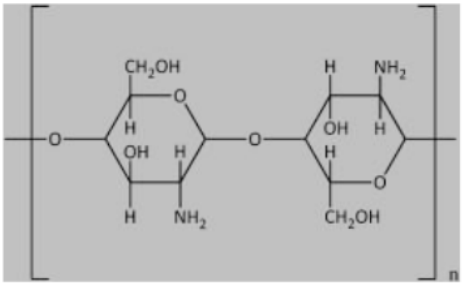

Fig. 1 The chemical structure of chitosan.

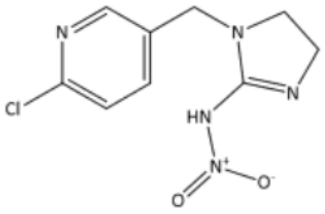

Fig. 2 The chemical structure of imidacloprid.

In this present paper, an attempt to enhance the controlled release properties of the zinc hydroxide nitrate–sodium dodecylsulphate–imidacloprid (ZHN–SDS–IC) nanocomposite was carried out by coating the ZHN–SDS–IC nanocomposite with chitosan (the coated nanocomposite will be denoted as ZHN–SDS–IC-Chi). Characterisation studies were subsequently performed on the ZHN–SDS–IC-Chi to examine the effect of the chitosan coating on the physicochemical properties of the nanocomposite. The controlled release study of ZHN–SDS–IC-Chi was investigated under similar experimental conditions as for ZHN–SDS–IC, and their release behaviour was then observed and compared. To the best of the authors' knowledge, no study has yet been reported on the potential of ZHN–SDS–IC-Chi as a CRF for a pesticide. A schematic representation of the present study is shown in Fig. 3.

2. Experimental

2.1 Materials

The $Zn(NO_3)_2$ $6H_2O$ (purity 98%) and SDS were purchased from Systerm (Malaysia). The IC that was intercalated in the interlayer gallery of ZHN–SDS was bought from Essense (China) with a purity of 98%. The glacial acetic acid and chitosan were supplied by Systerm (Malaysia) and Sigma Aldrich (USA) respectively.

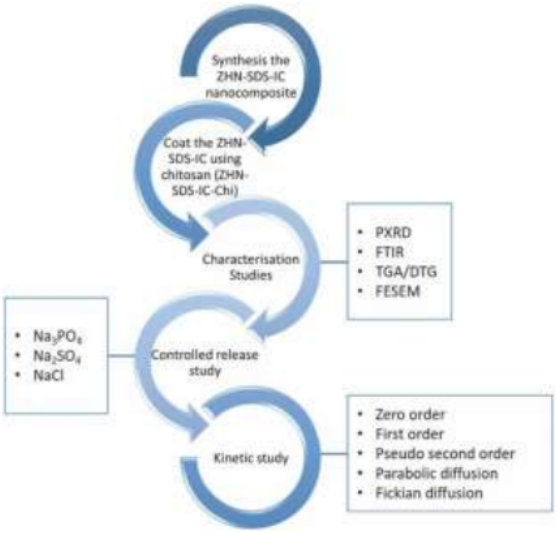

Fig. 3 The schematic representation of the study.

The release media were prepared using sodium phosphate (Na_3PO_4), sodium sulphate (Na_2SO_4) and sodium chloride (NaCl). The Na_3PO_4 (purity 99.5%) was supplied by Merck (Germany), whereas both the Na_2SO_4 (purity 95.2%) and NaCl (purity 99.0%) were purchased from Systerm (Malaysia). All reagents in the study were used as-received and without further purification. The deionised water was used as a solvent to prepare all solutions.

2.2 Synthesis of ZHN–SDS–IC, ZHN–SDS–Chi and ZHN–SDS–IC-Chi nanocomposites

The ZHN–SDS was prepared by co-precipitation using $Zn(NO_3)_2$ $6H_2O$ and SDS as the precursors. The ZHN–SDS–IC nanocomposite was then synthesised by mixing the ZHN–SDS into the IC solution and stirring constantly for 24 h. The procedure for the synthesis of the ZHN–SDS and ZHN–SDS–IC was described in a paper previously published by the authors.[31]

The synthesis of the chitosan coated ZHN–SDS–IC nanocomposite (denoted as ZHN–SDS–IC-Chi) was started by preparing the chitosan solution for the coating process. A quantity of 0.1 g chitosan was weighed and dissolved in 1% glacial acetic acid. As gelation of the chitosan began, it was heated for 30 minutes under magnetic stirring to dissolve the chitosan. Then, 50 mL of deionised water was added into the mixture and it was continuously stirred at room temperature for 24 h to completely dissolve the chitosan. Next, 0.1 g of the ZHN–SDS–IC nanocomposite was added into the mixture and it was continuously stirred for 18 h. The ZHN–SDS–IC-Chi nanocomposite was collected by centrifugation (4000 rpm for 5 min) and dried in an oven (at 60 1C for 24 h). The product was ground and kept in a sample bottle. The ZHN–SDS was also coated using a similar procedure, and it was denoted as ZHN–SDS–Chi.

2.3 Characterisation

Powder X-ray diffraction (PXRD) was carried out on a PANalytical X-pert Pro MPD diffractometer using Co K-alpha radiation (**l** = 1.54056 Å). The PXRD measurements were conducted at room temperature, with the Bragg angle ranging from 2 to 601, a scanning speed of 21 min ^{1}, step size of 0.03301 and scan step time of 9.4434 s. The PXRD instrument used an operating voltage and current of 40 kV and 30 mA, respectively. The Fourier transform infrared (FTIR) spectra were performed on a Nicolet FTIR spectrometer (400–4000 cm ^{1}). The nominal resolution of the FTIR was set to 4 cm ^{1} and the samples were compressed in a KBr disk with a mass ratio (sample/KBr) of 1 : 100. Thermal behaviour of the samples was studied by thermogravimetric analysis and differential thermal analysis (TGA/DTG). The measurements were performed on a Perkin-Elmer Pyris 1 TGA thermo balance in nitrogen gas at a heating rate of 10 1C min ^{1} and in the range 35–1000 1C. The surface morphology of the samples was probed using a field emission scanning electron microscope (FESEM, Hitachi SU 8020 UHR).

2.4 Controlled release formulation study of the ZHN–SDS–IC-Chi nanocomposite

The amount of IC that was released from the interlayer gallery of the ZHN–SDS–IC-Chi nanocomposite was measured by a Lambda 25 PerkinElmer ultraviolet-visible (UV/Vis) spectrometer ($\mathbf{l}_{max}$ = 269.5). The experimental conditions for the UV/Vis spectrometer included a time interval of 60 s, slit width of 1.0 nm, lamp change of 326.0 nm, ordinate max of 1.0 and ordinate min of 0.0. The release media were prepared using an aqueous solution of Na_3PO_4, Na_2SO_4 and NaCl, each prepared in three concentrations: 0.1 M, 0.3 M and 0.5 M. In each measurement, 0.6 mg of the ZHN–SDS–IC-Chi nanocomposite was released in 3.5 mL of release media and left for several days until the absorbance reading became constant. The accumulated percentage release of the IC was calculated using a standard calibration curve that was obtained from a series of standard solutions of IC. In order to understand the mechanism of release, the release data were then fitted into five kinetic models: zero order, first order, pseudo second order, parabolic diffusion and Fickian diffusion models. This was carried out so that the release mechanism could be examined in detail.

3. Results and discussion

3.1 PXRD analysis

The PXRD analysis was beneficial for determining the crystallinity of the nanocomposite before and after it was coated with chitosan.[23] The PXRD patterns of the chitosan, ZHN–SDS, ZHN–SDS–IC, ZHN–SDS–Chi and ZHN–SDS–IC-Chi are presented in Fig. 4. Based on the PXRD patterns, an obvious and broad peak, with basal spacing of 4.5 Å, was spotted in the PXRD pattern of the chitosan, indicating a typical amorphous structure. The amorphous peak of the chitosan is in good agreement with previous results in the literature.

The major characteristic peaks for the ZHN–SDS, with a basal spacing of 32.0 Å and 9.8 Å, were symmetrical, intense and sharp, thus signifying their highly crystalline nature. These peaks were also detected in the PXRD pattern for the ZHN–SDS (basal spacing of 33.4 Å and 10.0 Å) after it is coated with chitosan, although the intensity of the peaks was greatly reduced due to the presence of the amorphous chitosan. The presence of the chitosan in the ZHN–SDS–Chi was also confirmed and was based on the appearance of the characteristic peak of chitosan (basal spacing of 4.5 Å) in the PXRD pattern. The chitosan characteristic peak was also observed in the PXRD pattern for the ZHN–SDS–IC-Chi.

The ZHN–SDS–IC showed an intense intercalation peak at a lower angle of 2y, with basal spacing of 32.0 Å, 16.3 Å and 10.9 Å, owing to the presence of the well crystallized ZHN–SDS–IC. Similar peaks can also be seen in the PXRD pattern for the ZHN–SDS–IC-Chi (basal spacing of 32.5 Å, 16.2 Å and 10.9 Å). The intercalation peaks of the ZHN–SDS–IC-Chi overlapped with the noise that originated from the chitosan, which made it visibly less obvious compared to the peaks for the ZHN–SDS–IC nanocomposite. In fact, the amorphous chitosan coating process diminished the peaks and caused them to appear as flattened humps instead of as sharp peaks. The conversion from a well crystallized structure into an amorphous one provided additional

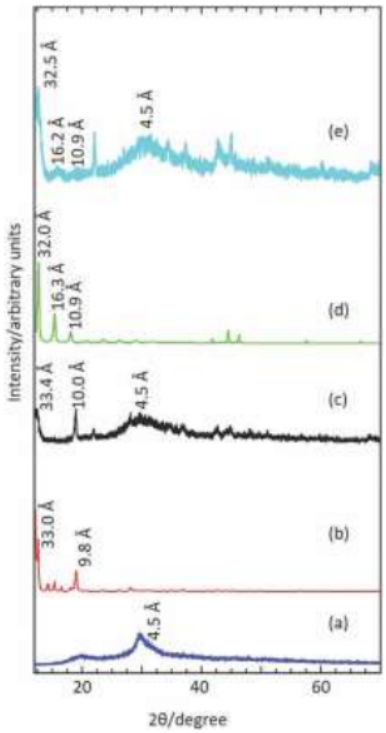

Fig. 4 PXRD patterns of (a) chitosan, (b) ZHN–SDS, (c) ZHN–SDS–Chi, (d) ZHN–SDS–IC[31] and (e) ZHN–SDS–IC-Chi.

evidence for the success of the chitosan coating of the ZHN–SDS–IC nanocomposite. The changes in the PXRD pattern after the chitosan coating are in good agreement with the previous study.[32,33]

The PXRD analysis also revealed that the chitosan coating process on both ZHN–SDS and the ZHN–SDS–IC did not cause any major changes in the interlayer distance. Although not all basal spacing values of the peaks in the PXRD pattern of the ZHN–SDS and the ZHN–SDS–IC remained exactly the same, the changes were very insignificant. Hence, this indicated that the chitosan coating process did not interfere with the ions intercalated in the interlayer gallery for both ZHN–SDS and ZHN–SDS–IC.

The ZHN–SDS–IC that was coated in this study was prepared using a similar concentration of IC (0.01 M), as this concentration was found to be the most optimum concentration to be intercalated into the ZHN–SDS system.[31] Both ZHN–SDS and the ZHN–SDS–IC synthesised were coated with chitosan, using a chitosan to nanocomposite mass ratio of 1 : 1. This composition was selected based on the good result obtained from the PXRD analysis as compared to the other ratio. Therefore, the composition was fixed throughout the study.

3.2 Spatial arrangement of the chitosan coated ZHN–SDS–IC nanocomposite

As mentioned in a previous paper by the authors, the height of the interlayer gallery of ZHN–SDS–IC was found to be 22.0 Å, whereas the dimensions of IC and SDS were calculated to be 12.5 9.2 7.2 Å and 19.9 6.1 5.2 Å, respectively (as predicted by Chem 3D Ultra 8.0 software).[31] Based on this information, the IC and SDS were believed to be oriented in the interlayer gallery of ZHN in a vertical monolayer arrangement.

In this present paper, it was found that after the ZHN–SDS–IC was coated with chitosan, the height of the interlayer gallery of the ZHN–SDS–IC increased slightly. The basal spacing of the ZHN–SDS–IC-Chi was determined to be 32.5 Å (provided by the PXRD analysis), the thickness of the ZHN was 4.8 Å and the thickness of the Zn tetrahedron was 2.6 Å. Therefore, the height of the interlayer gallery of the ZHN–SDS–IC-Chi was 22.5 Å, which is considerably greater for the ZHN–SDS–IC. The slight increment in the height of the interlayer gallery after the ZHN–SDS–IC was coated with chitosan was due to the ZHN–SDS–IC-Chi enabling the vertical monolayer arrangement. The proposed spatial arrangements of the ZHN–SDS–IC and the ZHN–SDS–IC-Chi nanocomposites are shown in Fig. 5.

3.3 FTIR analysis

In order to further investigate the impact of the chitosan coating on both ZHN–SDS and ZHN–SDS–IC, FTIR analysis was applied. The results obtained from the FTIR analysis are shown in Fig. 6 and also summarised inTable 1. In general, several typical characteristic peaks for the chitosan were observed in the FTIR spectra of chitosan at 1665 cm^{-1} (amide I), 1556 cm^{-1} (N–H bending) and 1052 cm^{-1} (C–N stretching from amide).[21–23,34] The broad peak that appeared from the stretching

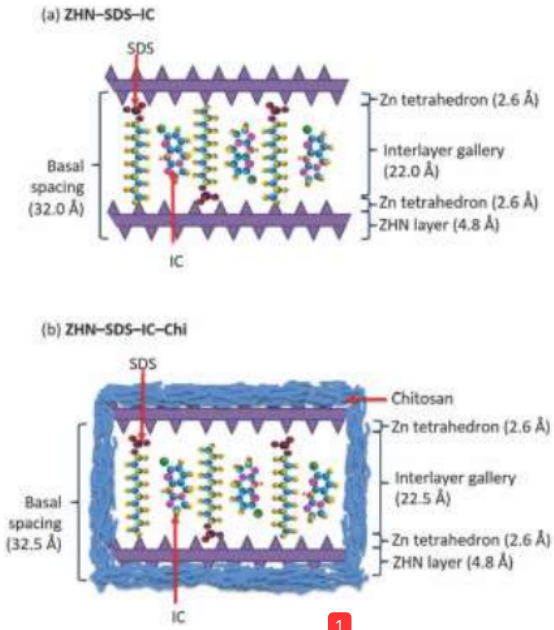

Fig. 5 Spatial orientation of IC and SDS in the interlayer gallery of (a) ZHN–SDS–IC[31] and (b) ZHN–SDS–IC-Chi.

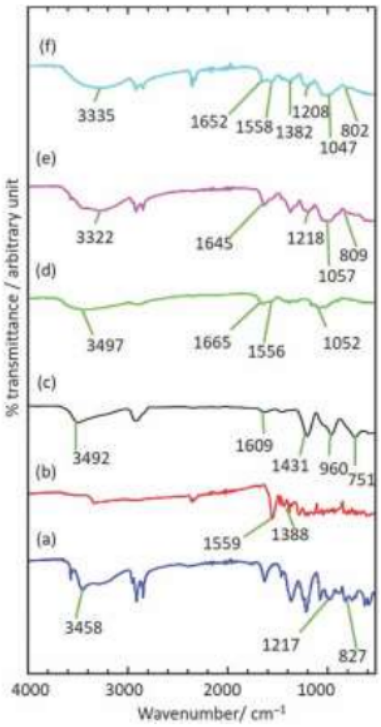

Fig. 6 FTIR spectra of (a) ZHN–SDS,[31] (b) IC,[31] (c) ZHN–SDS–IC,[31] (d) chitosan, (e) ZHN–SDS–Chi and (f) ZHN–SDS–IC-Chi.

of the hydroxyl group can be observed in the FTIR spectra of the ZHN–SDS, chitosan, ZHN–SDS–Chi, ZHN–SDS–IC and ZHN–SDS–IC-Chi at 3458 cm $^{-1}$, 3497 cm $^{-1}$, 3322 cm $^{-1}$, 3492 cm $^{-1}$ and 3335 cm $^{-1}$, respectively.

After the ZHN–SDS was coated with chitosan, several peaks that were attributed to SDS and chitosan can be seen in the FTIR spectra of the ZHN–SDS–Chi. The peaks that indicate the presence of SDS were observed at 1218 cm $^{-1}$ and 809 cm $^{-1}$ due to the asymmetric stretching of SQO and stretching of S–O, respectively.[35] These peaks were originally found in the FTIR spectra of the ZHN–SDS at 1217 cm $^{-1}$ and 827 cm $^{-1}$. The peak that indicated the presence of chitosan in the ZHN–SDS–Chi can be seen at 1645 cm $^{-1}$ and 1057 cm $^{-1}$ due to the amide I and C–N stretching, respectively.[21–23,34]

In the case of the ZHN–SDS–IC, the FTIR spectra of the ZHN–SDS–IC-Chi itself showed some features of IC, SDS and chitosan after it was coated. The characteristic peak for the IC that was attributed to the pyridine (originally found in the FTIR spectra of IC and ZHN–SDS–IC at 1559 cm $^{-1}$ and 1609 cm $^{-1}$, respectively) was also observed in the FTIR spectra of ZHN–SDS–IC-Chi at 1558 cm $^{-1}$.[35] The peak that signifies the N–O bond in the nitro group of IC can be observed in the FTIR spectra of the ZHN–SDS–IC-Chi at 1382 cm $^{-1}$ and also in both FTIR spectra of the IC and ZHN–SDS–IC at 1388 cm $^{-1}$ and 1431 cm $^{-1}$, respectively. The appearance of pyridine and N–O peaks therefore proves that the IC was loaded in both ZHN–SDS–IC and ZHN–SDS–IC-Chi. The characteristic peaks for SDS can be observed in the FTIR spectra of the ZHN–SDS–IC-Chi at 1208 cm $^{-1}$ (asymmetric stretching of SQO) and 802 cm $^{-1}$ (stretching of S–O). The characteristic peaks for chitosan were observed at 1652 cm $^{-1}$ (amide I) and 1047 cm $^{-1}$ (C–N stretching from amide).[21–23,34,36,37] Before the ZHN–SDS–IC underwent the chitosan coating process, the peaks that are assigned to the asymmetric stretching of SQO and S–O were previously observed in the FTIR spectra of ZHN–SDS–IC at 960 cm $^{-1}$ and 751 cm $^{-1}$, respectively.

All the aforementioned characteristic peaks that appeared in the FTIR spectra show that the chitosan coating did not affect the SDS and IC that were intercalated in the interlayer gallery of the ZHN–SDS. Hence, it can be concluded that the result obtained from the FTIR analysis is in good agreement with the PXRD analysis.

3.4 Thermal stability studies

The impact of the chitosan coating process on the thermal stability of ZHN–SDS and ZHN–SDS–IC was assessed using TGA/DTG. The difference in the weight loss of the samples was observed as a function of temperature in the range of 35–100 1C. The TGA/DTG curves that were obtained from the thermal stability studies of chitosan, ZHN–SDS–Chi and ZHN–SDS–IC-Chi are shown in Fig. 7.

Based on the TGA/DTG curves, all samples experienced multiple stages of thermal decomposition in the temperature range studied. The chitosan experienced three stages of weight loss (Fig. 7(a)), whereas the ZHN–SDS–Chi (Fig. 7(b)) and the ZHN–SDS–IC-Chi (Fig. 7(c)) experienced thermal decomposition in three and four stages of weight loss, respectively. These data were then summarised and compared with the data from

Table 1 FTIR spectra of ZHN–SDS, IC, ZHN–SDS–IC, chitosan, ZHN–SDS–Chi and ZHN–SDS–IC-Chi

Attribution	ZHN–SDS	IC	ZHN–SDS–IC	Chitosan	ZHN–SDS–Chi	ZHN–SDS–IC-Chi
n(O–H) in H_2O	3458	—	3492	3497	3322	3335
n_s(CQC) in amide I	—	—	—	1665	1645	1652
n_s(C–N) in amide	—	—	—	1556	—	—
n_s(C–O–C)	—	—	—	1052	1057	1047
n_{as}(SQO) in SDS	1217	—	960	—	1218	1208
n_s(S–O) in SDS	827	—	751	—	809	802
Pyridine in IC	—	1559	1609	—	—	1558
n_s(N–O) in IC	—	1388	1431	—	—	1382
Ref.	31	31	31	Present paper	Present paper	Present paper

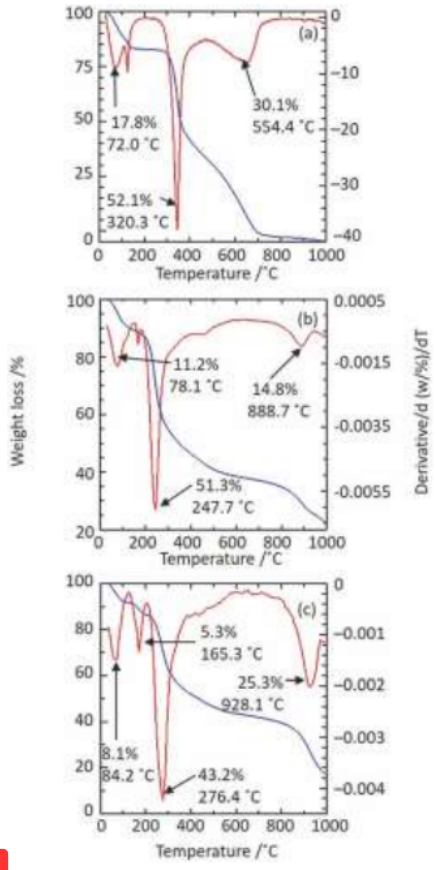

Fig. 7 TGA/DTG curves of (a) chitosan, (b) ZHN–SDS–Chi and (c) ZHN–SDS–IC-Chi nanocomposites.

the thermal stability study of the uncoated samples of ZHN–SDS and ZHN–SDS–IC that were reported in the authors' previous paper (Table 2).[31]

During the thermal decomposition of chitosan, the first weight loss occurred at 72.0 1C, with 17.8% of weight loss; the second weight loss occurred at 320.3 1C, with an abrupt weight loss of 52.1%; and the third weight loss took place at 554.4 1C, with 30.2% of weight loss. A significant change in the thermal behaviour of the ZHN–SDS was observed after it was coated with chitosan. Before the ZHN–SDS chitosan coating process, the thermal decomposition occurred in two stages. The first stage occurred at 107.1 1C with 3.2% of weight loss due to the loss of adsorbed and wa[3] molecules. The second stage occurred at 198.2 1C with 37.2% of weight loss due to the decomposition of SDS.[38] After the ZHN–SDS was coated with chitosan, the thermal decomposition occurred in three stages. Similar to the ZHN–SDS, the first thermal decompositions of ZHN–SDS–Chi were attributed to the loss of water which occurred at 78.1 1C with a weight loss of 11.2%. The second thermal decomposition which occurred at 247.7 1C with a weight loss 51.3%, was due to the dehydration of the saccharide rings and the depolymerisation of the chitosan. The attainment of chitosan as a coating material to enhance thermal stabilities was revealed based on the appearance of an additional thermal decomposition peak in the TGA/DTG curve of the ZHN–SDS–Chi that indicates the combustion of SDS and the collapsing of the layered structure occurred at a significantly high temperature (888.7 1C with 14.8% of weight loss).

The TGA/DTG curve for the ZHN–SDS–IC nanocomposite showed four stages of thermal decomposition at 108.1 1C (6.2% of weight loss), 166.4 1C (31.2% of weight loss), 264.2 1C (3.3% of weight loss) and 595.2 1C (14.3% of weight loss). The loss of sample weight at 108.1 1C was related to the elimination of adsorbed and structural water molecules, whereas the weight loss at 166.4 1C could be ascribed to the decomposition of the intercalated IC. The weight loss that occurred at 264.2 1C was due to the combustion of SDS that was present in the interlayer gallery of the ZHN–SDS–IC. The last weight loss occurred at 595.2 1C as the layered structure collapsed. The thermal decomposition of ZHN–SDS–IC-Chi also occurred in four stages at 84.0 1C (8.2% of weight loss), 165.3 1C (5.3% of weight loss), 276.2 1C (43.6% of weight loss) and 928.1 1C (25.4% of weight loss), which was attributed to similar thermal events as in the ZHN–SDS–IC nanocomposite. Although the temperatures for the first three stages of the thermal decomposition of the ZHN–SDS–IC and ZHN–SDS–IC-Chi were not very different, it should be pointed out that a drastic change can be observed in the temperature for the fourth stage of thermal decomposition. The temperature of the fourth stage of thermal decomposition for the ZHN–SDS–IC-Chi (928.1 1C) was much higher than for the ZHN–SDS–IC (595.2 1C). This indicated a better thermal stability

Table 2 TGA/DTG data of weight loss for chitosan, ZHN–SDS, ZHN–SDS–Chi, ZHN–SDS–IC and ZHN–SDS–IC-Chi

Thermal decomposition		Samples				
		Chitosan	ZHN–SDS	ZHN–SDS–Chi	ZHN–SDS–IC	ZHN–SDS–IC-Chi
Stage 1	T_{max} (1C)	72.0	107.1	78.1	108.1	84.0
	Percentage (%)	17.8	3.2	11.2	6.2	8.2
Stage 2	T_{max} (1C)	320.3	198.2	247.7	166.4	165.3
	Percentage (%)	52.1	37.2	51.3	31.2	5.3
Stage 3	T_{max} (1C)	554.4	—	888.7	264.2	276.2
	Percentage (%)	30.1	—	14.8	3.3	43.6
Stage 4	T_{max} (1C)	—	—	—	595.2	928.1
	Percentage (%)	—	—	—	14.3	25.4
Ref.		Present paper	31	Present paper	31	Present paper

for the ZHN–SDS–IC-Chi. The major change indicated that the prominent protective effect of the chitosan on the thermal decomposition of the ZHN–SDS–IC was similar to ZHN–SDS. The potential of chitosan to enhance the thermal stability of both ZHN–SDS–Chi and ZHN–SDS–IC-Chi is in good agreement with previous studies in the literature.[23,32,34]

3.5 Surface morphology analysis

The chitosan, ZHN–SDS, ZHN–SDS–Chi, ZHN–SDS–IC and ZHN–SDS–IC-Chi nanocomposites were subjected to surface morphology analysis using FESEM, as shown in Fig. 8. The FESEM micrographs revealed a total surface morphological transformation of the ZHN–SDS and ZHN–SDS–IC after both samples underwent the chitosan coating process.

Before the ZHN–SDS was coated with chitosan, it had a typical morphology of a layered material, with a tabular, stacked plate-like structure and sharp edges. After it was coated with chitosan, its former plate-like structure was no longer observable. The chitosan caused the ZHN–SDS–Chi to have a surface morphology that resembled the surface morphology of the chitosan. As for the ZHN–SDS–IC, the surface morphology showed that before it was coated with the chitosan, it had a thin plate-like structure with rounded edges. The chitosan coating seemed to flatten out the surface of the ZHN–SDS–IC-Chi, causing the surface to be more compact and resembling the surface morphology of the pure chitosan. The results obtained from the surface morphology showed that the chitosan coating process greatly affected the surface morphology of both the ZHN–SDS and ZHN–SDS–IC nanocomposites.

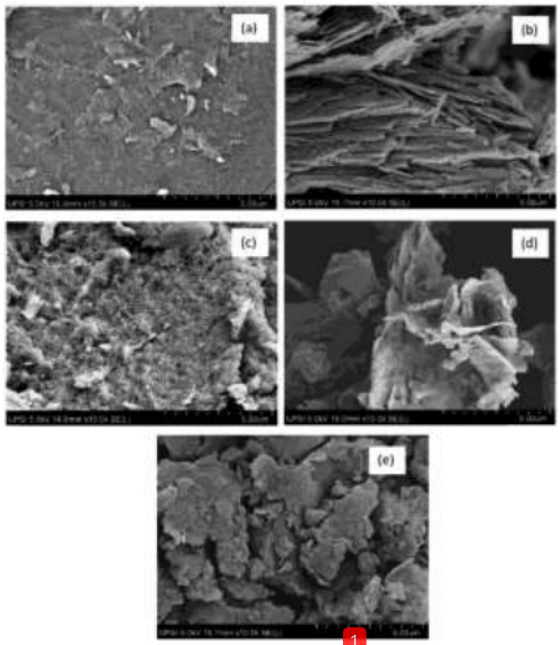

Fig. 8 Surface morphology of (a) chitosan, (b) ZHN–SDS, (c) ZHN–SDS–Chi, (d) ZHN–SDS–IC and (e) ZHN–SDS–IC-Chi.

3.6 Release study of ZHN–SDS–IC-Chi into single, binary and ternary systems of aqueous solutions

The release behaviour of the intercalated ion was influenced by the size of the nanocomposite, the properties of the reactants and the nature of the interactions.[39] Here, the impact of the chitosan coating on the release behaviour of the IC was investigated by performing the release study of the ZHN–SDS–IC-Chi nanocomposite using various concentrations of Na_3PO_4, Na_2SO_4 and NaCl as the release media. The release profile for the IC from the ZHN–SDS–IC-Chi is shown in Fig. 9. The percentage releases of IC from ZHN–SDS–IC (based on the authors' previous paper) and ZHN–SDS–IC-Chi into single, binary and ternary systems of aqueous solutions were also compared, so that the effect of the chitosan coating on the release of IC in a release medium containing multiple types of anion can be observed (Table 3).

As shown in Fig. 9, the release behaviour of the IC from the interlayer gallery of the ZHN–SDS–IC-Chi nanocomposite was strongly dependent on the nature of the release media. The release in Na_3PO_4, exhibited the highest level of cumulative release, with 96%, followed by Na_2SO_4 and NaCl, with 87% and 86%, respectively. A higher affinity for the trivalent PO_4^{3-} anions present in the Na_3PO_4 increased the tendency of the PO_4^{3-} to be attracted to the positively charged ZHN, and this eased the ion exchange process between the PO_4^{3-} and the IC. A similar trend for the release as for the ZHN–SDS–IC was observed when the concentration of the release media varied. This indicated that the release of the IC from the interlayer gallery of ZHN–SDS–IC-Chi was also concentration-dependent. The percentage of release was greater in a higher concentration of the release media, and it decreased when the release was

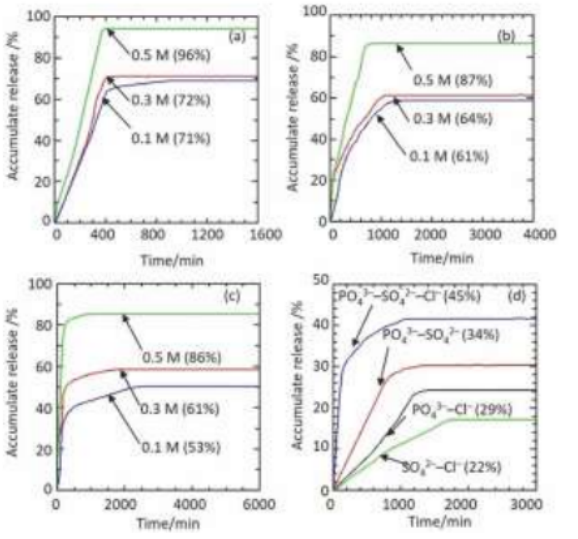

Fig. 9 Release profiles of IC from ZHN–SDS–IC-Chi nanocomposite into (a) sodium phosphate, (b) sodium sulphate, (c) sodium chloride solution in various concentrations and (d) mixture aqueous solution of phosphate, sulphate and chloride in several combinations.

Table 3 Comparison of the release time of IC from ZHN–SDS–IC and ZHN–SDS–IC-Chi into single, binary and ternary aqueous systems of phosphate, sulphate and chloride

Aqueous solutions			ZHN–SDS–IC		ZHN–SDS–IC-Chi	
			Percentage release (%)	Release time (hour)	Percentage release (%)	Release time (hour)
Single	PO_4^{3-}	0.1 M	29	5.2	71	14.7
		0.3 M	74	2.9	72	6.7
		0.5 M	91	1.4	96	6.5
	SO_4^{2-}	0.1 M	16	11.5	61	21.6
		0.3 M	83	7.9	64	17.2
		0.5 M	86	5.0	87	13.0
	Cl^-	0.1 M	6	24.6	53	41.1
		0.3 M	84	13.2	61	28.9
			85	9.2	86	16.7
		0.5 M	83	22.0	34	21.8
Binary	PO_4^{3-} –SO_4^{2-}		25	23.0	29	23.6
	PO_4^{3-} –Cl^-		22	23.8	22	28.8
	SO_4^{2-} –Cl^-		84	11.9	45	18.1
Ternary	PO_4^{3-} –SO_4^{2-} –Cl^-		31			
Ref.					Present paper	

performed in a lower concentration of the release media. In the release study that was performed in the aqueous solution of Na_3PO_4, the cumulative percentages released when using 0.5 M, 0.3 M and 0.1 M were 96%, 72% and 71%, respectively. The cumulative percentages released in aqueous Na_2SO_4 were 87%, 64% and 61%. When the release was performed in aqueous NaCl, the cumulative percentages released were 86.2%, 60.8% and 53.1%, respectively. This is because as more anions were supplied in the release media at a higher concentration, it was easier for the ion exchange to occur.[40]

The release process that was performed in the aqueous solution containing Cl^- took the longest time to reach its maximum release, and the order was $Cl^- < SO_4^{2-} < PO_4^{3-}$. This could be predominantly attributed to the low charge density of the Cl^- anions, which made it less attracted to the ZHN layer compared to the other anions and allowed the release process.[40–42] The time taken for IC to be released from the interlayer gallery of ZHN–SDS–IC-Chi was also concentration-dependent. The release in the 0.5 M, 0.3 M and 0.1 M of aqueous NaCl required release times of 41.1 hours, 28.9 hours, and 16.7 hours, respectively. As for the release in 0.5 M, 0.3 M and 0.1 M of aqueous Na_2SO_4, the release times needed were 21.6 hours, 17.2 hours and 13.0 hours, respectively. Whereas for the 0.5 M, 0.3 M and 0.1 M of aqueous NaCl, the times needed for the release were 14.7 hours, 6.7 hours and 6.5 hours, respectively. Even though the release patterns for the ZHN–SDS–IC-Chi and ZHN–SDS–IC were quite similar, the release time for the ZHN–SDS–IC-Chi was significantly longer compared to the ZHN–SDS–IC nanocomposite. The significant increase in the release time for the IC after the ZHN–SDS–IC was coated with chitosan demonstrates the potential of a chitosan coating in sustaining the release of IC.

In the release study of IC from the ZHN–SDS–IC-Chi nanocomposite into the binary and ternary systems of aqueous solutions, the highest percentage of accumulated release of IC was observed in the aqueous solution containing PO_4^{3-} –SO_4^{2-} –Cl^-, followed by PO_4^{3-} –SO_4^{2-}, PO_4^{3-} –Cl^- and SO_4^{2-} –Cl^-, with percentages of 45%, 34%, 29% and 22%, respectively. In terms of their percentage release, the presence of chitosan somehow leads to a reduction in terms of their percentage release. This trend was also similar to those reported in several previous studies that used polysaccharides as the coating material.[34,43–45] It is also noticeable that the times needed to release IC into the binary and ternary systems of aqueous solutions were found to be significantly extended after undergoing the chitosan coating process, regardless of their anion combination. The release process of IC in the ternary system of PO_4^{3-} –SO_4^{2-} –Cl^- demonstrates the shortest release time (18.1 hours) amongst all release media containing multiple types of anions, hence indicating that the release process in this mixture has the fastest release. As for the release in the aqueous solutions of PO_4^{3-} –SO_4^{2-} and PO_4^{3-} –Cl^-, the times required to achieve the maximum percentage of accumulated release of IC are 21.8 hours and 23.6 hours, respectively. The slowest release was obtained when the release process was performed in the aqueous solution containing SO_4^{2-} –Cl^- with a release time of 28.8 hours. These changes show that the presence of chitosan leads to the gradual release of IC in multiple anions, hence proving the potential of chitosan in improving the controlled release behaviour of the ZHN–SDS–IC nanocomposite.

Coincident with the result obtained in this study, previous studies also pointed out the potential of chitosan in slowing the release rate of intercalated ions from their host.[22,39,46] The polycationic nature of the chitosan plays a significant role in decelerating the release rate of ZHN–SDS–IC-Chi. The positively charged amino groups on the backbone of the chitosan are capable of forming electrostatic interactions with the anionic SDS surfactant, and hence strengthen the electrostatic attractions that formerly existed between the SDS and the ZHN layers. Owing to the fact that the neutral charge IC exists in the hydrophobic region created by the SDS as micelles, the stronger electrostatic attractions formed result in the SDS and IC being held more tightly in the interlayer gallery of the ZHN–SDS–IC-Chi nanocomposite, thus increasing the time taken for the ion exchange process to occur between the anionic SDS surfactant and IC, with the incoming anions in the release media. The impact of the polycationic properties of chitosan in slowing the release of an intercalated guest ion is in good agreement with previous studies.[24,26,34,47–50]

Due to the hydrophilic nature of chitosan, the release of the intercalated IC from the hydrophilic matrices of chitosan is influenced by the rate of the matrix hydration and the gelation ability of the chitosan matrix.[51] The gelation ability of the chitosan is also due to its hygroscopic nature, which permits the chitosan to have a greater ability to form hydrogen bonds with water.[52] These properties considerably affect the ion diffusion, gel formation and erosion of the chitosan matrix.[53] Other than slowing the release rate of the intercalated ion from its host, the gelation ability of the chitosan also assisted in reducing the burst release phenomenon for the release behaviour of the IC from the ZHN–SDS–IC-Chi. A significant reduction in the burst release was most obvious when the

Na_3PO_4 was used as the release media. As can be seen from the release profile, no abrupt release was observed during the initial part of the release, which indicated that the release process occurred in a sustained manner from the very beginning. Fast hydration allowed the formation of a gel layer and prevented the excessive release of the intercalated ions that was caused by the burst release during the early part of the release process.[53] Based on the release profile, it can be deduced that the chitosan coating immediately swelled when the nanocomposite was immersed in the release media, followed by subsequent gel layer formation and a gradual release of the IC. Hence, the results from the release study proved that the ZHN–SDS–IC-Chi is suitable for controlling the release of IC and the chitosan coating formulation was beneficial for increasing the CRF properties of the ZHN–SDS–IC nanocomposite.

3.7 Kinetic study of IC from the ZHN–SDS–IC-Chi nanocomposite into various aqueous solutions

To obtain a deeper understanding on the release mechanism of the IC from the interlayer gallery of the ZHN–SDS–IC-Chi nanocomposite, the data collected in the release studies were fitted into several kinetic models that were zero order, first order, pseudo second order, parabolic diffusion and Fickian diffusion kinetic models. The fitting of the release data on the kinetic models are shown in Fig. 10–12. The correlation coefficient (r^2), rate constant (k) and half time ($t_{1/2}$) were obtained from the fitting and are summarised in Table 4.

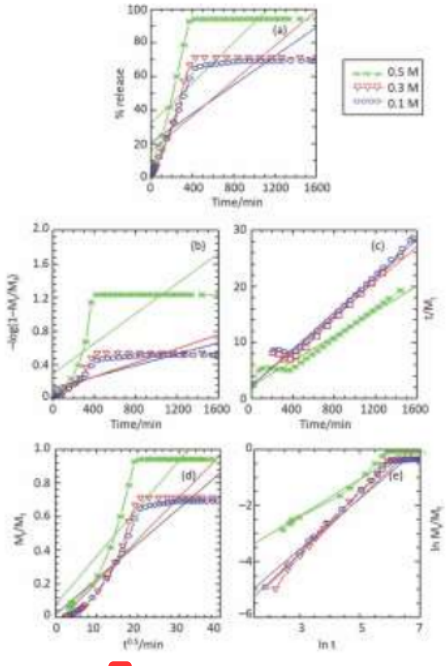

Fig. 10 Fitting of the data for IC release from the ZHN–SDS–IC-Chi nanocomposite into sodium phosphate solution for the (a) zero order, (b) first order, (c) pseudo second order, (d) parabolic diffusion and (e) Fickian diffusion models.

Table 4 Comparison of rate constants, k, and regression values, r^2, obtained from the fitting of the data of release from ZHN–SDS–IC-Chi into aqueous solutions of Na_3PO_4, Na_2SO_4 and NaCl

Aqueous solution		Zero order	First order	Parabolic diffusion	Fickian diffusion	Pseudo second order		
		r^2	r^2	r^2	r^2	r^2	k (10^{-3} s^{-1})	$t_{1/2}$
Na_3PO_4	0.1 M	0.670	0.716	0.850	0.970	0.983	0.052	243.5
	0.3 M	0.687	0.720	0.868	0.966	0.969	0.055	227.9
	0.5 M	0.633	0.678	0.972	0.826	0.972	0.062	204.5
Na_2SO_4	0.1 M	0.556	0.591	0.841	0.864	0.870	0.041	304.4
	0.3 M	0.539	0.584	0.874	0.987	0.993	0.054	234.2
	0.5 M	0.479	0.544	0.882	0.779	0.957	0.050	249.8
NaCl	0.1 M	0.491	0.551	0.683	0.710	0.997	0.098	128.8
	0.3 M	0.414	0.461	0.643	0.834	1.000	0.113	111.2
	0.5 M	0.319	0.389	0.505	0.582	0.999	0.143	87.8

As can be seen in Fig. 10–12, the plot of t/M_t against t/M_i shows the best fit for the release data. This indicates that the release of IC from the interlayer gallery of ZHN–SDS–IC-Chi in all release media is in good agreement with the pseudo second order kinetic model. The summarised release data in Table 4 show that the r^2 values obtained are the highest (closest to 1) when the data were fitted into the pseudo second order kinetic model. The r^2 values obtained for the release study in the aqueous solutions of Na_3PO_4, Na_2SO_4 and NaCl are $r^2 = 0.969$, $r^2 = 870$ and $r^2 = 0.997$, respectively. The linearization of the release data into other kinetic models (zero order, first order, parabolic diffusion and Fickian diffusion) was unsatisfactory because the release data were poorly fitted and resulted in low r^2 values.

The release behaviour of IC from the interlayer gallery of ZHN–SDS–IC-Chi can also be interpreted in terms of the $t_{1/2}$ values, which represent the time needed to reach half of the maximum accumulated release of the intercalated IC. The changes of the $t_{1/2}$ values in all release media seemed to share a similar trend, where the $t_{1/2}$ values in all release media decreased as the concentration of the release media increased. This is because the release media with a higher concentration provided more ions, and hence more ions were available for the release process.[40] The higher concentration accelerated the release process and consequentially lowered the $t_{1/2}$ values for the release process.

The release behaviour for the IC that was governed by the pseudo second order kinetic model indicated that the release process started through dissolution and was subsequently followed by an ion exchange process.[54] The hygroscopic nature and gelation properties of the chitosan enabled the chitosan to form a gel layer that protected the outer surface of the ZHN–SDS–IC nanocomposite and sustained the release of IC from the nanocomposite.[45,52] The interaction between the chitosan gel layer and the water molecule in the release media hydrated the chitosan gel layer and caused the gel layer to swell. As more water penetrated into the gel layer, the swelling increased and triggered the slow dissolution of the gel layer at the ZHN–SDS–IC nanocomposite. This allowed the slow release of the intercalated IC into the release media. A further dissolution

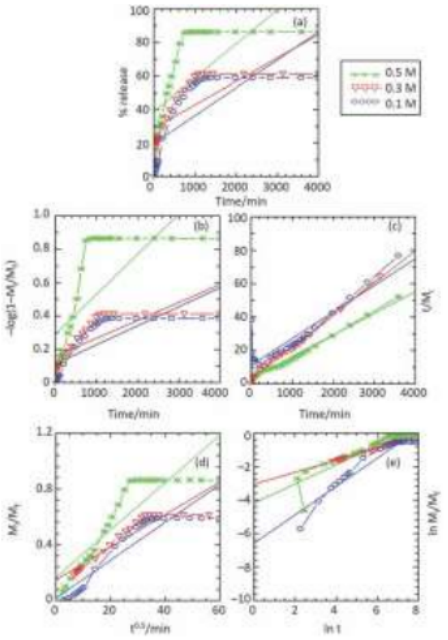

Fig. 11 Fitting of the data for IC release from the ZHN–SDS–IC-Chi nanocomposite into sodium sulphate solution for the (a) zero order, (b) first order, (c) pseudo second order, (d) parabolic diffusion and (e) Fickian diffusion models.

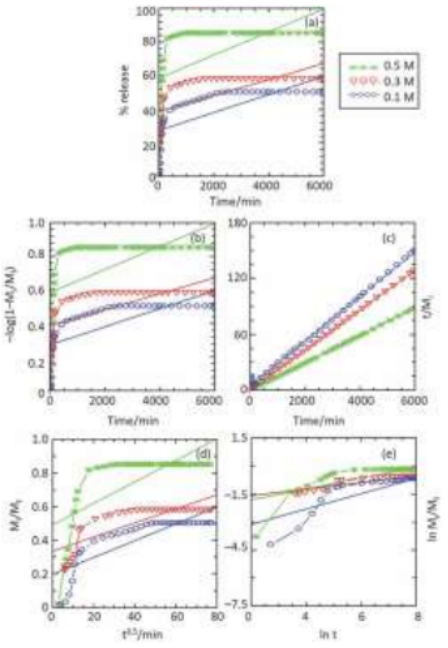

Fig. 12 Fitting of the data for IC release from the ZHN–SDS–IC-Chi nanocomposite into sodium chloride solution for the (a) zero order, (b) first order, (c) pseudo second order, (d) parabolic diffusion and (e) Fickian diffusion models.

process deteriorated the chitosan gel layer and the ZHN–SDS–IC nanocomposite and initiated the occurrence of the release process via ion exchange.

Based on the release study, it can be concluded that the release mechanisms for the ZHN–SDS–IC and ZHN–SDS–IC-Chi nanocomposites were quite similar. Both cases were governed by the pseudo second order model, which indicated that the release process occurred via dissolution and ion exchange. However, a significant improvement in the CRF properties of the ZHN–SDS–IC nanocomposite was observed after it was coated with chitosan. The coating process generated the formation of a chitosan gel layer that contributed to slowing the release process and increasing the $t_{1/2}$ values.

4. Conclusions

Even though there are numerous previous studies that reported on the CRF of pesticides, most of the pesticides use in the system exist in anionic nature. A neutral charge guest ion may not be directly intercalated into the interlayer gallery of layered metal hydroxides owing to the neutral charge possessed by this ion. As a result of their challenging intercalation process, fewer studies have reported on the CRF of neutral charge pesticides, as compared to the anionic pesticides. The results reported in this work demonstrate the success of the chitosan coating on the ZHN–SDS–IC nanocomposite in a simple, easy and less time-consuming process, as an endeavour for enhancing the CRF of neutral charge pesticides. The characterisation study performed using PXRD and FTIR revealed that the chitosan process did not interfere with the types of ions intercalated in the ZHN–SDS–IC nanocomposite. A slight increase in the interlayer gallery height allowed the ZHN–SDS–IC-Chi nanocomposite to preserve its vertical monolayer arrangement. The chitosan coating process was proven to increase the thermal stability of the ZHN–SDS–IC-Chi nanocomposite and transform its surface morphology into a flatter and more compact plate-like structure. The results from the release study provided insight into the suitability of chitosan to be used as a coating material and its potential to prolong the release of the intercalated IC from the ZHN–SDS–IC nanocomposite. The highest percentage of cumulative release was observed when the ZHN–SDS–IC-Chi nanocomposite was immersed in aqueous solutions of Na_3PO_4, in the order of Na_3PO_4 → Na_2SO_4 → NaCl. The slowest release process was observed when NaCl was used as the release media, and the release process was also found to be concentration-dependent. The enhancement in the release behaviour of the ZHN–SDS–IC-Chi nanocomposite was due to the hydrophilic and hygroscopic nature of chitosan, which made it possible for the chitosan to form a gel layer in the hydrated environment. The kinetic study showed that the release of IC from the ZHN–SDS–IC-Chi was governed by the pseudo second order model and indicated that the release mechanism was via dissolution and the ion exchange process. It is always worthwhile to give an extra effort to develop a new pesticide that satisfies both economic and ecological demand.

Thus, the potential of chitosan to enhance the controlled release properties of ZHN–SDS–IC-Chi can hopefully help to reduce the risk of pollution due to the excessive use of pesticides in the agricultural sector.

Conflicts of interest

None declared.

Acknowledgements

The authors wish to thank UPSI and Ministry of Education Malaysia for the support during completing the research. This work was supported by the GPU-RISING STAR Grant No. 2019-0119-103-01.

Notes and references

1 S. Kumaran, A. Kamari, M. M. Abdulrasool, S. T. S. Wong, J. Jumadi, S. N. M. Yusoff and S. Ishak, J. Phys.: Conf. Ser., 2019, 1397, 012030.
2 S. N. M. Yusoff, A. Kamari, S. Ishak, J. Jumadi, M. M. Abdulrasool, S. Kumaran and S. T. S. Wong, J. Phys.: Conf. Ser., 2019, 1397, 012026.
3 I. N. F. A. Aziz, S. H. Sarijo, F. S. M. R. Y. Rajidi and M. Musa, J. Porous Mater., 2019, 26, 717–722.
4 M. Z. Hussein, N. F. Nazarudin, S. H. Sarijo and M. A. Yarmo, J. Nanomater., 2012, 1–10.
5 G. Gwak, S. Paek and J. Oh, Eur. J. Inorg. Chem., 2012, 5269–5275.
6 A. Matalanis, O. G. Jones and D. J. McClements, Food Hydrocolloids, 2011, 25, 1865–1880.
7 Q. Z. Yang, Y. Y. Chang and H. Z. Zhao, Water Res., 2013, 47, 6712–6718.
8 J. Liu, X. Zhang and Y. Zhang, ACS Appl. Mater. Interfaces, 2015, 7, 11180–11188.
9 R. Otero, J. M. Fernández, M. A. Ulibarri, R. Celis and F. Bruna, Appl. Clay Sci., 2012, 65–66, 72–79.
10 L. M. Varca, Agric. Water Manag., 2012, 106, 35–41.
11 G. Preetha, J. Stanley, S. Suresh and R. Samiyappan, Chemosphere, 2010, 80, 498–503.
12 M. Z. Bin Hussein, A. H. Yahaya, Z. Zainal and L. H. Kian, Sci. Technol. Adv. Mater., 2005, 6, 956–962.
13 S. Dubey, V. Jhelum and P. K. Patanjali, J. Sci. Ind. Res., 2011, 70, 105–112.
14 A. M. Bashi, M. Z. Hussein, Z. Zainal and D. Tichit, J. Solid State Chem., 2013, 203, 19–24.
15 M. Z. Hussein, N. S. S. A. Rahman, S. H. Sarijo and Z. Zainal, Int. J. Mol. Sci., 2012, 13, 7328–7342.
16 M. Z. Hussein, N. Hashim, A. H. Yahaya and Z. Zainal, Solid State Sci., 2010, 12, 770–775.
17 S. M. N. Mohsin, M. Z. Hussein, S. H. Sarijo, S. Fakurazi, P. Arulselvan and T.-Y. Y. Hin, Chem. Cent. J., 2013, 7, 26.
18 N. Hashim, Z. Muda, S. A. Hamid, I. Isa, A. Kamari, A. Mohamed, Z. Hussein and S. A. Ghani, J. Phys. Chem. Sci., 2014, 1, 1–6.
19 M. Z. bin Hussein, M. Y. Ghotbi, A. H. Yahaya and M. Z. Abd Rahman, Mater. Chem. Phys., 2009, 113, 491–496.
20 B. Saifullah, M. Z. Hussein, S. H. Hussein-Al-Ali, P. Arulselvan and S. Fakurazi, Chem. Cent. J., 2013, 7, 72.
21 E. Corradini, M. R. De Moura and L. H. C. Mattoso, eXPRESS Polym. Lett., 2010, 4, 509–515.
22 Y. Luo, Z. Teng, Y. Li and Q. Wang, Carbohydr. Polym., 2015, 122, 221–229.
23 S. A. Agnihotri and T. M. Aminabhavi, J. Controlled Release, 2004, 96, 245–259.
24 I. Alemzadeh and M. Vossoughi, Chem. Eng. Process., 2011, 41, 707–710.
25 K. Nakagawa, N. Sowasod, W. Tanthapanichakoon and T. Charinpanitkul, LWT – Food Sci. Technol., 2013, 54, 600–605.
26 S. Woranuch and R. Yoksan, Carbohydr. Polym., 2013, 96, 578–585.
27 I. Ishaaya and A. R. Horowitz, in Insecticides with novel modes of action, ed. I. Ishaaya and D. Degheele, Springer, Berlin, Heidelberg, 1998, pp. 1–24.
28 S. Hervé Thany, Insect Nicotinic Acetylcholine Receptors, 2010.
29 I. Yamamoto and J. E. Casida, Nicotinoid Insecticides and the Nicotinic Acetylcholine Receptor, 1999.
30 S. Jorgen, Chemical Pesticides Mode of Action and Toxicology, CRC Press, Boca Raton, 2004.
31 S. N. M. Sharif, N. Hashim, I. M. Isa, S. A. Bakar, M. I. Saidin, M. S. Ahmad, M. Mamat and M. Z. Hussein, J. Porous Mater., 2020, 27, 473–486.
32 Y. Luo, T. T. Y. Wang, Z. Teng, P. Chen, J. Sun and Q. Wang, Food Chem., 2013, 139, 224–230.
33 Z. Teng, Y. Luo and Q. Wang, J. Agric. Food Chem., 2012, 60, 2712–2720.
34 S. F. Hosseini, M. Zandi, M. Rezaei and F. Farahmandghavi, Carbohydr. Polym., 2013, 95, 50–56.
35 D. P. Qiu, W. G. Hou, J. Xu, J. Liu and S. Liu, Chin. J. Chem., 2009, 27, 1879–1885.
36 M. Li, S. Chen, F. Ni, Y. Wang and L. Wang, Electrochim. Acta, 2008, 53, 7255–7260.
37 Q. Tao, J. Yuan, R. L. Frost, H. He, P. Yuan and J. Zhu, Appl. Clay Sci., 2009, 45, 262–269.
38 N. Hashim, S. N. M. Sharif, Z. Muda, I. M. Isa, N. M. Ali, S. A. Bakar, S. M. Sidik and M. Z. Hussein, Mater. Res. Innovations, 2018, 23, 233–245.
39 R. Grillo, A. E. S. Pereira, C. S. Nishisaka, R. De Lima, K. Oehlke, R. Greiner and L. F. Fraceto, J. Hazard. Mater., 2014, 278, 163–171.
40 S. Li, Y. Shen, M. Xiao, D. Liu and L. Fan, Arabian J. Chem., 2015, 12, 2563–2571.
41 S. A. I. S. M. Ghazali, M. Z. Hussein and S. H. Sarijo, Nanoscale Res. Lett., 2013, 8, 1–8.
42 S. H. Sarijo, S. A. I. S. M. Ghazali, M. Z. Hussein and A. H. Ahmad, Mater. Today: Proc., 2015, 2, 345–354.
43 Z. Rezvani and M. Shahbaei, Polym. Compos., 2014, 36, 1819–1825.
44 L. N. M. Ribeiro, A. C. S. Alcântara, M. Darder, P. Aranda, F. M. Araújo-Moreira and E. Ruiz-Hitzky, Int. J. Pharm., 2014, 463, 1–9.
45 N. B. Allou, A. Yadav, M. Pal and R. L. Goswamee, Carbohydr. Polym., 2018, 186, 282–289.

46 B. P. Koppolu, S. G. Smith, S. Ravindranathan, S. Jayanthi, T. K. Suresh Kumar and D. A. Zaharoff, Biomaterials, 2014, 35, 4382–4389.
47 C. Sanjai, S. Kothan, P. Gonil, S. Saesoo and W. Sajomsang, Carbohydr. Polym., 2014, 104, 231–237.
48 J. D. Bumgardner, A. Des Rieux, N. Duhem, J. Dutta, P. K. Dutta, T. Furuike, C. Gao, W. O. Haggard, R. Jayakumar, J. A. Jennings, C. Jerome, M. R. Leedy, X. Liu, L. Ma, Z. Mao, H. J. Martin, R. A. A. Muzzarell, P. A. Norowski, N. Nwe, M. Prabaharan, V. Preat, H. Ragelle, K. Rinki, R. Riva and H. Tamura, Advances in Polymer Science, Springer-Verlag, Berlin Heidelberg, London, 2011.
49 D. Davidson and F. X. Gu, J. Agric. Food Chem., 2012, 60, 870–876.
50 M. Vemmer and A. V. Patel, Biol. Control, 2013, 67, 380–389.
51 J. Nunthanid, M. Laungtana-Anan, P. Sriamornsak, S. Limmatvapirat, S. Puttipipatkhachorn, L. Y. Lim and E. Khor, J. Controlled Release, 2004, 99, 15–26.
52 E. Szymańska and K. Winnicka, Mar. Drugs, 2015, 13, 1819–1846.
53 R. M. Lucinda-Silva, H. R. N. Salgado and R. C. Evangelista, Carbohydr. Polym., 2010, 81, 260–268.
54 N. Hashim, Z. Muda, S. A. Hamid, I. M. Isa, A. Kamari, A. Mohamed, M. Z. Hussein and S. A. Ghani, J. Phys. Chem. Sci., 2014, 1, 1–6.

The impact of a hygroscopic chitosan coating on the controlled release behaviour of zinc hydroxide nitrate–sodium dodecylsulphate–imidacloprid nanocomposites

ORIGINALITY REPORT

10%	9%	10%	2%
SIMILARITY INDEX	INTERNET SOURCES	PUBLICATIONS	STUDENT PAPERS

PRIMARY SOURCES

1	Hani Masitah MadJin, Norhayati Hashim, Illyas Md Isa, Mohd Zobir Hussein et al. "Synthesis and characterisation of zinc hydroxides nitrates–sodium dodecyl sulphate fluazinam nano hosts for release properties", Journal of Porous Materials, 2020 Publication	3%
2	Submitted to School of Business and Management ITB Student Paper	2%
3	Norhayati Hashim, Sharifah Norain Mohd Sharif, Illyas Md Isa, Shahidah Abdul Hamid et al. "Controlled release formulation of an anti-depression drug based on a L-phenylalanate-zinc layered hydroxide intercalation compound", Journal of Physics and Chemistry of Solids, 2017 Publication	2%
4	doaj.org Internet Source	2%

5	www.researchgate.net Internet Source	2%

Exclude quotes	On	Exclude matches	< 80 words
Exclude bibliography	On		